

Article

Influence of the Reaction Conditions in the Crystal Structures of Zn(II) and Ni(II) Coordination Compounds with a Dissymmetric Bis(Thiosemicarbazone) Ligand

Luis Alonso, Rodrigo Burón, Elena López-Torres * and Maria Antonia Mendiola *

Departamento de Química Inorgánica, Universidad Autónoma de Madrid, Cantoblanco, 28049 Madrid, Spain; luis.alonso@estudiante.uam.es (L.A.); rodrigo.buron@estudiante.uam.es (R.B.)

* Correspondence: elena.lopez@uam.es (E.L.-T.); antonia.mendiola@uam.es (M.A.M.); Tel.: +34-914-972-376 (E.L.-T.); +34-914-974-844 (M.A.M.)

Abstract: The new ligand HMeATSM, derived from condensation of 2-3-butanedione with 4-methyl-3-thiosemicarbazide and 2,4-dimethyl-3-thiosemicarbazide, has been synthesized. Its reactivity with nickel(II) and zinc(II) nitrates was explored and the resulting complexes were thoroughly characterized by elemental analysis, conductivity, mass spectrometry, IR, ^1H and ^{13}C NMR spectroscopies and their structures were confirmed by single-crystal X-ray diffraction. The results showed that the complex $[\text{Ni}(\text{MeATSM})]\text{NO}_3$ 1 is formed under every reaction condition. In contrast, the reaction with zinc(II) nitrate depends on the temperature and the presence of $\text{LiOH}\cdot\text{H}_2\text{O}$, leading to the obtaining of complexes $[\text{Zn}(\text{MeATSM})(\text{OH}_2)](\text{NO}_3)$ 2 and $[\text{Zn}(\text{Me}_2\text{TS})_2(\text{OH}_2)](\text{NO}_3)_2$ 3. The crystal structures of complexes 1 and 2 show that the dissymmetric ligand acts as a N_2S_2 tetradentate monoanionic ligand. The structural preferences of the metals also determine the structure of the complexes: whereas nickel(II) is in a square-planar environment, the zinc atom prefers a distorted square-base pyramid geometry imposed by the coordination mode and the planarity of the bis(thiosemicarbazone) ligand. In contrast, in complex 3, containing two bidentate Me_2TS ligands, the Zn(II) is in a trigonal bipyramid arrangement. In all the complexes, the nitrate ion is not coordinated to the metal and acts as a counterion.

Keywords: thiosemicarbazones; X-ray diffraction; nickel complexes; zinc complexes

Citation: Alonso, L.; Burón, R.; López-Torres, E.; Mendiola, M.A. Influence of the Reaction Conditions in the Crystal Structures of Zn(II) and Ni(II) Coordination Compounds with a Dissymmetric Bis(Thiosemicarbazone) Ligand. *Crystals* **2022**, *12*, 310. <https://doi.org/10.3390/cryst12030310>

Academic Editor: Scott J. Dalgarno

Received: 2 February 2022

Accepted: 17 February 2022

Published: 23 February 2022

Publisher's Note: MDPI stays neutral with regard to jurisdictional claims in published maps and institutional affiliations.



Copyright: © 2022 by the authors. Licensee MDPI, Basel, Switzerland. This article is an open access article distributed under the terms and conditions of the Creative Commons Attribution (CC BY) license (<https://creativecommons.org/licenses/by/4.0/>).

1. Introduction

The structure of coordination compounds, both from a molecular and supramolecular point of view, has a direct influence on their properties, so it is very important to understand how we can modulate or control the architectures of those systems. Synthetically, we can rationally design the ligands incorporating the most suitable binding groups, taking into account metal preferences such as coordination geometries and for hard or soft donor atoms. However, there are other factors that can also be controlled, such as ligand deprotonation, the use of anions with different donor abilities or reaction conditions such as temperature or solvent. Although sometimes the reactivity can be somehow predicted, in many other cases this may be challenging, especially if polydentate ligands with several groups that can be deprotonated are used.

The kind of ligands that can perfectly fit this approach are thiosemicarbazones (TSCs). The main advantages of these donor systems are the presence of both hard (N) and soft (S) donor atoms and the possibility of acting as neutral or anionic donor due to NH deprotonation. This confers to these ligands a huge versatility in terms of coordination modes [1,2]. The most common one is as N,S bidentate chelate [3,4], coordination mode that affords the formation of a very stable five-membered chelate ring, but many others are described in the literature, for example S monodentate [5,6], N,S bidentate chelate and S bridge [7,8]

or N,S bidentate chelate and N bridge [9]. This, together with the control of protonation/deprotonation and the nature of auxiliary anions, lead to the formation of different structures such as monomers [10–12], dimers [13–15] or coordination polymers [16–18]. In addition to their fascinating structural properties, TSCs have a wide range of applications in different fields as catalysis [19–21], metal detoxification [22–24], metal sensing [25–27] or medicine [28–31].

Following our interest in the chemistry of TSC ligands [32–35], in this paper we report the synthesis and structure of a dissymmetric bis(TSC) ligand and its complexes with Ni(II) and Zn(II), as well as a compound isolated after ligand decomposition. The compounds are characterized by several spectroscopic techniques as well as by single-crystal X-ray diffraction. The synthesis of dissymmetric ligands is always complicated, since the symmetrical [1 + 2] or the cyclic [1 + 1] molecules are usually more stable than the dissymmetric ones. In addition, even if the ligand is successfully isolated, symmetrization or decomposition can take place, as evidenced in the results presented in this article.

2. Materials and Methods

2.1. Measurements

Microanalyses were carried out using a LECO CHNS-932 Elemental Analyzer. IR spectra in the 4000–400 cm^{-1} range were recorded as KBr pellets on a Jasco FT/IR-410 spectrophotometer. The ESI mass spectra in positive mode were recorded on a Q-STAR PULSAR I instrument using a hybrid analyzer QTOF (Quadrupole time-of-flight). ^1H and ^{13}C NMR spectra were recorded on a spectrometer Bruker AVIII HD-300 MHz using DMSO- d_6 as solvent and TMS as internal reference. ^{13}C CP/MAS NMR spectra were recorded at 298 K in a Bruker AV400WB spectrometer equipped with a 4 mm MAS (magnetic angle spinning) NMR probe and obtained using a cross polarization pulse sequence using spinning rates of 10–14 KHz, pulse delay of 30 s, contact times of 8 ms and TPPM (two-pulse phase-modulated) high-power proton decoupling. Chemical shifts are reported relative to TMS and the CH of adamantane (29.5 ppm) as a secondary reference. Conductivity was measured using a freshly prepared DMF solution (ca. 10^{-3} M) at 25 °C with a Crison EC-Meter BASIC 30+ instrument. Magnetic susceptibilities were collected on a Sherwood Scientific balance at room temperature.

Crystallographic data were collected on a Bruker Kappa Apex II diffractometer equipped with an Apex-II CCD area detector using a graphite monochromator (Mo k_α radiation, $\lambda = 0.71073$ Å). The substantial redundancy in data allows empirical absorption corrections (SADABS) [36] to be applied using multiple measurements of symmetry-equivalent reflections. The raw intensity data frames were integrated with the SAINT program, which also applied corrections for Lorentz and polarization effects [37]. The software package SHELXTL version 6.10 was used for space group determination, structures solution and refinement. The structures were solved by direct methods (SHELXS-97) [38], completed with difference Fourier syntheses, and refined with full-matrix least squares using SHELXL 2014 minimizing $\omega(F_0^2 - F_c^2)$. Weighted R factors (R_w) and all goodness of fit S area based on F^2 ; conventional R factors (R) are based on F [39]. All non-hydrogen atoms were refined with anisotropic displacements parameters. The hydrogen atoms bonded to carbon atoms were positioned geometrically and those on nitrogen and oxygen atoms were located in a difference Fourier map and their coordinates and isotropic thermal parameters subsequently refined.

CCDC numbers 2149688–2149691 for the ligand and complexes 1–3, respectively, contain the supplementary crystallographic data for this paper. These data can be obtained free of charge via <http://www.ccdc.cam.ac.uk/conts/retrieving.html> accessed on 1 February 2022 (or from the CCDC, 12 Union Road, Cambridge CB2 1EZ, UK; Fax: +44 1223 336033; E-mail: deposit@ccdc.cam.ac.uk).

2.2. Starting Materials

All the chemicals were purchased from standard commercial sources and used without further purification.

2.3. Synthesis of the Organic Molecules

2.3.1. Synthesis of 2,4-Dimethyl-3-Thiosemicarbazide, Me₂TS

In total, 2.00 g (41.2 mmol) of methylhydrazine was dropwise added to a solution of 3.00 g (41.0 mmol) of methylisothiocyanate in 50 mL of diethyl ether cooled in an ice bath. The mixture was stirred for one hour and the white solid formed was filtered off, washed several times with diethyl ether and dried under vacuum (yield 92%). Elemental analysis calc for C₃H₉N₃S (%): C, 30.24; H, 7.62; N, 35.29; S, 26.86. Found: C, 29.98; H, 7.59; N, 35.04; S, 26.71. IR (KBr, cm⁻¹): 3315s, 3265s, 3176m (NH), 1633s (δNH₂), 1527s (thioamide I+CN), 877s (thioamide IV). ¹H NMR (DMSO-d₆) 8.09 (H_{6a}, 1H, d, ³J = 3.2 Hz), 4.77 (NH₂, 2H, s), 3.30 (H₉, 3H, s), 2.85 (H₆, 3H, d, ³J = 4.6 Hz).

2.3.2. Synthesis of Diacetyl-2-(4-Methyl-3-Thiosemicarbazone), HAME₂S

In total, 10.50 mL (119.7 mmol) of 2,3-butanodione (diacetyl) was added to a solution of 4.07 g (39.9 mmol) of 4-methyl-3-thiosemicarbazide (MeTS) in water and the mixture was stirred at room temperature for 1.5 h. The white solid formed was filtered off, washed several times with cold water and dried under vacuum (yield 89%). Elemental analysis calc for C₃H₁₁N₃OS (%): C, 26.26; H, 8.08; N, 30.63; S, 23.37. Found: C, 25.98; H, 8.01; N, 30.35; S, 23.24. ESI⁺ *m/z* 174.1 [M+H]⁺ IR (KBr, cm⁻¹): 3324s, 3290s, (NH), 1673s (CO), 1636w, 1594s, 1542vs (thioamide I+CN), 836m (thioamide IV). ¹H NMR (DMSO-d₆) 10.60 (H₂, 1H, s), 8.60 (H_{1a}, 1H, d, ³J = 4.4 Hz), 3.10 (H₁, 3H, d, ³J = 4.6 Hz), 2.40 (H₈, 3H, s), 1.90 (H₇, 3H, s). ¹³C NMR (DMSO-d₆): 197.4 (CO), 178.9 (C₂), 145.4 (C₃), 31.3 (C₁), 24.7 (C₈), 9.9 (C₇).

2.3.3. Synthesis of

Diacetyl-(2,4-Dimethylthiosemicarbazone)-2-(4-Methyl-3-Thiosemicarbazone), HMeATSM

A solution of 0.88 g (7.8 mmol) of Me₂TS in 10 mL of dry methanol was added to 0.68 g (3.9 mmol) of HAME₂S in 20 mL of dry methanol. The mixture was stirred at room temperature for one hour. The pale-yellow solid formed was filtered off, washed with methanol and dried under vacuum (yield 97%). Elemental analysis calc for C₉H₁₈N₆S₂ (%): C, 39.40; H, 6.62; N, 30.52; S, 23.33. Found: C, 39.22; H, 6.50; N, 30.56; S, 23.39. IR (KBr, cm⁻¹): 3331s, 3300s, (NH), 1588w, 1531vs, 1497vs (thioamide I + CN), 832m (thioamide IV). ¹H NMR (DMSO-d₆) 10.50 (H₂, 1H, s), 8.40 (H₁, 1H, q, ³J = 4.4 Hz), 7.52 (H₆, 1H, q, ³J = 4.2 Hz), 3.40 (H_{9a-c}, 3H, s), 3.03 (H_{1a-c}, 3H, d, ³J = 4.3 Hz), 2.90 (H_{6a-c}, 3H, d, ³J = 4.4 Hz), 2.18, 2.17 (H_{7a-c}, 3H, s + H_{8a-c}, 3H, s). ¹³C NMR (DMSO-d₆): 180.9 (C₅), 179.3 (C₂), 169.6 (C₄), 147.6 (C₃), 41.8 (C₉), 32.7 (C₆), 31.7 (C₁), 15.6 (C₈), 12.6 (C₇). ¹³C NMR (CP/MAS): 178.6 (C₅), 175.1 (C₂), 148.0, 146.0 (C₄ + C₃), 42.7 (C₉), 33.5 (C₆), 32.0 (C₁), 15.8 (C₈), 12.4 (C₇). Yellow crystals for X-ray analysis were formed after slow evaporation of the mother liqueur.

2.4. Synthesis of Complexes

2.4.1. Synthesis of [Ni(MeATSM)]NO₃ (1)

A solution of 0.18 g (0.6 mmol) of nickel(II) nitrate hexahydrate in 15 mL of ethanol was added to a suspension of 0.15 g (0.6 mmol) of HMeATSM in 15 mL of ethanol and immediately the yellow mixture turns to brown. The mixture was stirred at room temperature for one hour, then the brown solid was filtered off, washed with ethanol and dried in vacuum (yield 86%). Elemental analysis calc for C₉H₁₇N₇O₃S₂Ni (%): C, 27.36; H, 4.60; N, 24.83; S, 16.20. Found: C, 27.32; H, 4.50; N, 24.81; S, 16.07. ESI⁺ *m/z* 331.0 [Ni(MeATSM)]⁺. μ (Scm²/mol, DMF): 65.5. IR (KBr, cm⁻¹): 3224s, (NH), 1592vs, 1565vs, 1492vs (thioamide I+CN), 827m (thioamide IV). ¹H NMR (DMSO-d₆) 10.30 (H₁, 1H, s), 8.10 (H₆, 1H, q, ³J = 4.5 Hz), 3.50 (H_{9a-c}, 3H, s), 2.85 (H_{6a-c}, 6H, d, ³J = 4.6 Hz), 2.24, 2.03 (H_{7a-c}, 3H, s + H_{8a-c}, 3H, s). ¹³C NMR (DMSO-d₆): 182.9 (C₅), 177.3 (C₂), 164.0 (C₄), 156.4 (C₃), 45.5 (C₉), 32.9 (C₆), 33.1 (C₁), 19.2 (C₈), 14.7 (C₇). Crystals suitable for single-crystal X-ray

diffraction were obtained by recrystallization in a mixture of ethanol/water 1:1. The same complex was obtained, but with lower yield (50%), in the presence of one equivalent of lithium hydroxide monohydrate.

2.4.2. Synthesis of $[\text{Zn}(\text{MeATSM})(\text{OH}_2)]\text{NO}_3$ (2)

A solution of 0.27 g (0.9 mmol) of zinc(II) nitrate hexahydrate in 3 mL of ethanol was added to a suspension of 0.24 g (0.9 mmol) of HMeATSM and 0.04 g (0.9 mmol) of lithium hydroxide monohydrate in 15 mL of ethanol and the mixture was stirred at room temperature for 24 h. The scarce amount of solid was filtered off and discarded and the solution was slowly evaporated until yellow crystals suitable for single-crystal X-ray diffraction were obtained (yield 65%). Elemental analysis calc for $\text{C}_9\text{H}_{19}\text{N}_7\text{O}_4\text{S}_2\text{Zn}$ (%): C, 25.81; H, 4.58; N, 23.42; S, 15.28. Found: C, 25.66; H, 4.53; N, 23.38; S, 15.24. $\text{ESI}^+ m/z$ 335.0 $[\text{Zn}(\text{MeATSM})]^+$. μ (Scm²/mol, DMF): 67.5. IR (KBr, cm⁻¹): 3332s, 3207m, 3100m (NH), 1583m, 1570w, 1564m, 1520m (thioamide I + CN), 836m (thioamide IV). ¹³C NMR (CP/MAS): 185.0 (C₅), 181.6 (C₂), 163.7, 146.1 (C₄ + C₃), 43.1 (C₉), 33.0 (C₆), 30.9 (C₁), 20.9 (C₈), 17.5 (C₇). In the absence of lithium hydroxide monohydrate the reagents were recovered.

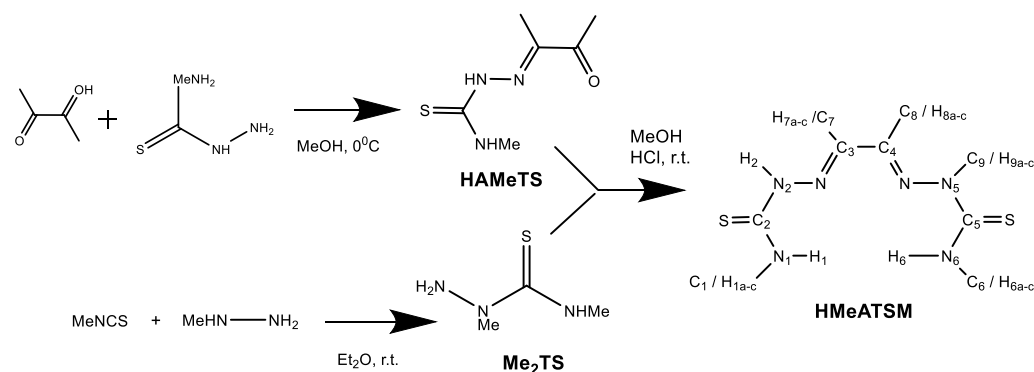
2.4.3. Synthesis of $[\text{Zn}(\text{Me}_2\text{TS})_2(\text{OH}_2)](\text{NO}_3)_2$ (3)

Following the procedure described for the synthesis of 2, but heating the mixture for 2 h, a white solid was obtained, which was filtered, washed with ethanol and vacuum dried (yield 35%). Elemental analysis calc for $\text{C}_6\text{H}_{20}\text{N}_8\text{O}_7\text{S}_2\text{Zn}$ (%): C, 16.16; H, 4.52; N, 25.14; S, 14.38. Found: C, 16.17; H, 4.45; N, 25.23; S, 14.35. μ (Scm²/mol, DMF): 117.2. IR (KBr, cm⁻¹): 3267s, 3160s (NH), 1571s (δ_{NH_2} + thioamide I), 824m (thioamide IV). ¹H NMR (DMSO-d₆) 8.10 (H₆, 1H, q, ³J = 4.5 Hz), 4.85 (NH₂, 2H, s), 3.41 (H_{9a-c}, 3H, s), 2.85 (H_{6a-c}, 3H, d, ³J = 4.4 Hz). ¹³C NMR (DMSO-d₆): 181.2 (C₅), 30.2 (C₆), 41.3 (C₉). The same complex was formed under reflux in the absence of lithium hydroxide monohydrate (yield 36%) and was also obtained by direct synthesis from Me₂TS and zinc(II) nitrate hexahydrate stirring at room temperature for one hour (yield 66%).

3. Results and Discussions

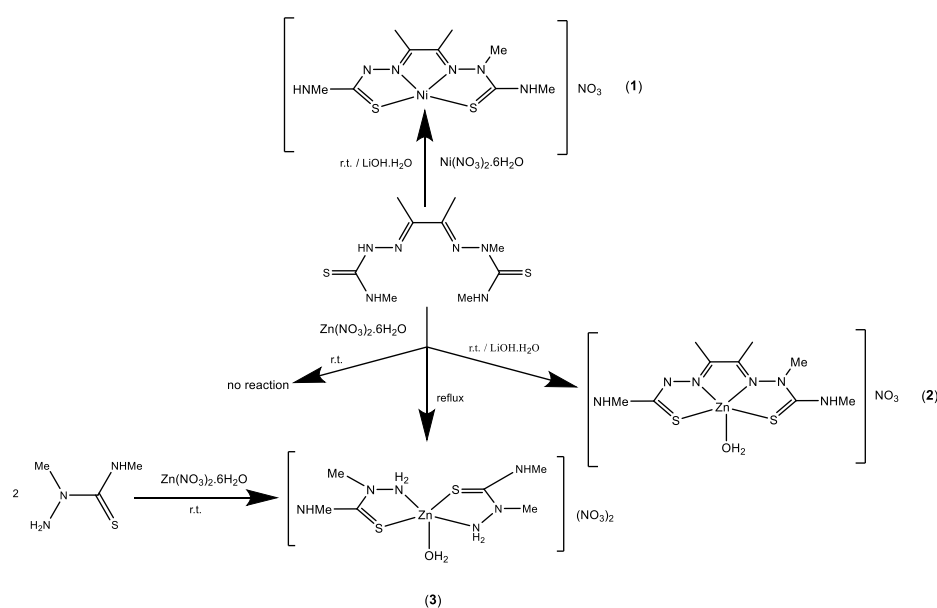
3.1. Synthesis

A new dissymmetric bis(thiosemicarbazone) ligand HMeATSM was synthesized by reaction of 2,4-dimethylthiosemicarbazide (Me₂TS) with diacetyl-2-(4-methyl-3-thiosemicarbazone), HAmETS. The synthesis of the monothiosemicarbazone HAmETS was achieved following the procedure previously reported in the literature by the group [16]. The condensation of Me₂TS with the residual carbonyl group of HAmETS was carried out with a 2:1 molar ratio (Scheme 1) to prevent the symmetrization reaction, since with 1:1 stoichiometry H₂ATSM was obtained.



Scheme 1. Synthesis of the ligand HMeATSM.

Reactions with the metal nitrates were carried out in ethanol, both in the absence and in the presence of one equivalent of lithium hydroxide monohydrate (Scheme 2). With nickel(II), all the reaction conditions yielded complex $[\text{Ni}(\text{MeATSM})]\text{NO}_3$ 1, with the ligand singly deprotonated. However, reactions with zinc(II) afforded different complexes depending on the presence of base and the temperature. At room temperature without base the reagents were recovered, but in the presence of base, complex $[\text{Zn}(\text{MeATSM})(\text{OH}_2)]\text{NO}_3$ 2 was obtained. In contrast, if the mixture was heated under reflux, with or without base, complex $[\text{Zn}(\text{Me}_2\text{TS})_2(\text{OH}_2)](\text{NO}_3)_2$ 3 was isolated, due to a symmetrization reaction to give H_2ATSM and Me_2TS . This complex can also be synthesized by reaction with Me_2TS at room temperature. This reactivity confirms the difficulty of working with dissymmetric ligands and proves that, even when the ligand is isolated, a symmetrization reaction can take place at any step of the complex formation, so control of the reaction conditions is essential.



Scheme 2. Synthesis of the coordination compounds.

The analytical data of complexes 1 and 2 confirm a 1:1 ligand to metal stoichiometry and the presence of a nitrate group; thus, the ligand acts as a monoanionic donor in both complexes. However, complex 3 is in agreement with a 1:2 Zn:ligand stoichiometry and the presence of two nitrate groups, so Me_2TS behaves as a neutral ligand. The mass spectra of complexes 1 (Figure S4) and 2 (Figure S7) only show the peak corresponding to the molecular ion, confirming the proposed stoichiometry. For both peaks, the found and calculated isotopic patterns are identical. Conductivity values in DMF for complexes 1 and 2 correspond to 1:1 electrolytes, and complex 3 is in agreement with a 1:2 electrolyte [40], showing that in the three complexes the nitrate groups act as counterions.

3.2. Crystal Structures

The molecular structures of HMeATSM and the three complexes have been determined by single-crystal X-ray diffraction. Significant crystal structure and refinement data are listed in Table 1 and relevant bond distances in the thiosemicarbazone skeleton and in the metal coordination environment are summarized in Tables 2 and 3, respectively. For the complexes, the different degrees of deprotonation of the ligands, together with the presence of one or two nitrate groups and the water molecules bonded to the zinc, make possible the existence of different supramolecular architectures based on different hydrogen bond arrays.

Table 1. Crystal data and structure refinements parameters for HMeATSM and complexes 1. H₂O, 2 and 3.

Compound	HMeATSM	1. H ₂ O	2	3
Empirical formula	C ₉ H ₁₈ N ₆ S ₂	NiC ₉ H ₁₉ N ₇ O ₄ S ₂	ZnC ₉ H ₁₉ N ₇ O ₄ S ₂	ZnC ₆ H ₂₀ N ₈ O ₇ S ₂
Formula weight	274.41	412.14	418.80	445.79
Crystal system	Triclinic	Monoclinic	Monoclinic	Monoclinic
Space group	P-1	P2(1)/n	P2(1)/n	C2/c
a/Å	7.6648(5)	7.0335(3)	8.3270(2)	18.7868(5)
b/Å	9.5516(6)	20.9318(6)	9.4816(3)	7.6851(2)
c/Å	9.8740(6)	11.6271(4)	21.9498(7)	13.3178(4)
α/°	89.227(3)	90	90	90
β/°	68.306(3)	103.110(2)	76.974(3)	120.374(2)
γ/°	85.152(3)	90	92.567(2)°	90
Volume/Å ³	669.16(7)	1667.17(10)	1237.95(15)	1731.27(9)
Z	2	4	2	4
Density (calculated)/Mg/m ³	1.362	1.642	1.607	1.785
Absorption coefficient mm ⁻¹	0.387	1.444	4.500	4.894
F(000)	292	856	864	920
GOF	1.151	1.118	1.063	1.173
Reflections collected	31,283	20,749	15,964	7988
Independent reflections	3568 [R(int) = 0.0353]	3272 [R(int) = 0.0508]	3296 [R(int) = 0.0365]	1564 [R(int) = 0.0412]
Final R indices [I > 2σ(I)]	R1 = 0.0414 wR2 = 0.1067	R1 = 0.0357 wR2 = 0.0948	R1 = 0.0432 wR2 = 0.1127	R1 = 0.0333 wR2 = 0.0841
Largest diff. peak and hole/e.Å ⁻³	0.586 and -0.306	0.531 and -0.825	1.821 and -0.737	0.581 and -0.332

Table 2. Selected bond distances (Å) for HMeATSM, 1. H₂O, 2 and 3.

	HMeATSM	1. H ₂ O	2	3
M(1)–N(3)	–	1.850(3)	2.110(3)	2.209(2)
M(1)–N(4)	–	1.867(3)	2.151(3)	–
M(1)–S(1)	–	2.1454(10)	2.3459(9)	2.3209(6)
M(1)–S(2)	–	2.1383(10)	2.3714(9)	–
M(1)–O(4)	–	–	2.006(2)	–
M(1)–O(1)	–	–	–	2.024(3)
C(2)–S(1)	1.6804(19)	1.756(4)	1.731(3)	1.719(2)
N(1)–C(2)	1.322(3)	1.336(5)	1.340(4)	1.329(3)
N(2)–C(2)	1.371(2)	1.328(4)	1.347(4)	1.340(3)
N(2)–N(3)	1.359(2)	1.375(4)	1.363(4)	1.419(3)
N(3)–C(3)	1.288(2)	1.294(5)	1.290(4)	–
N(4)–C(4)	1.288(2)	1.301(5)	1.281(4)	–
N(4)–N(5)	1.432(2)	1.391(4)	1.390(4)	–
N(5)–C(5)	1.358(3)	1.364(5)	1.368(4)	–
C(5)–N(6)	1.335(3)	1.311(5)	1.313(4)	–
C(5)–S(2)	1.6956(19)	1.722(4)	1.716(3)	–

Figure 1 shows the molecular structure of HMeATSM. It crystallizes in the triclinic P-1 space group. The compound is in the thione form, which is supported by the C-S bond distances (Table 2), which are intermediate between those of single and double bonds (1.82 and 1.56, respectively) and the presence of the hydrazinic hydrogen H₂. The azomethine bonds are 1.2888(2), which is in agreement with double bonds and the N–N bonds are shorter than 1.44 Å, which agrees well with those of similar thiosemicarbazones. The two arms of the molecule are *E* with respect to the single bond C(3)–C(4) and both azomethine nitrogen atoms N(3) and N(4) are in *E* with respect to the sulfur atoms Figures S1 and S2, which is the conformation usually found in the solid state for these kind of molecules [41,42]. The ligand is not planar and the two arms form an angle of 73.51°. The molecules are held together in the crystal packing through an extended network of intermolecular hy-

drogen bonds involving the amine nitrogen atoms N(1) and N(6) and the sulfur atoms S1 and S2 giving chains along the *c* axis.

Table 3. Selected bond angles ($^{\circ}$) for complexes 1. H₂O, 2 and 3.

	1. H ₂ O	2	3
N(3)–M(1)–S(1)	87.55(10)	81.90(7)	81.41(5)
N(3)#1–Zn(1)–S(1)	–	–	101.18(5)
N(3)#1–Zn(1)–N(3)	–	–	173.73(12)
S(1)–Zn(1)–S(1)#1	–	–	132.00(3)
O(1)–Zn(1)–N(3)	–	–	86.86(6)
O(1)–Zn(1)–S(1)	–	–	114.001(17)
O(4)–M(1)–N(3)	–	103.62(10)	–
O(4)–M(1)–N(4)	–	95.60(10)	–
N(3)–M(1)–N(4)	83.62(13)	73.72(10)	–
O(4)–M(1)–S(1)	–	104.83(8)	–
N(4)–M(1)–S(1)	170.36(10)	151.28(8)	–
O(4)–M(1)–S(2)	–	104.59(8)	–
N(3)–M(1)–S(2)	172.72(10)	142.65(7)	–
N(4)–M(1)–S(2)	89.35(10)	79.62(7)	–
S(1)–M(1)–S(2)	99.34(4)	113.48(3)	–

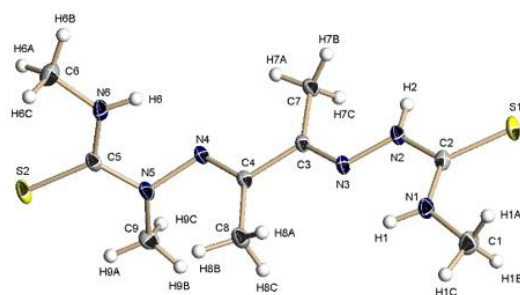


Figure 1. Molecular structure of HMeATSM. Thermal ellipsoids at 50% probability level.

Figure 2 represents the molecular structure of complex 1. It crystallizes with a water molecule in the monoclinic P2(1)/*n* space group. The asymmetric unit contains a single [Ni(MeATSM)]⁺ cation, a nitrate group as counterion and a water molecule of crystallization. The nickel(II) ion is coordinated to a N₂S₂ tetradentate anionic ligand. The pseudomacrocyclic coordination mode of the ligand affords three five-member chelate rings that confer high stability to the complex. The value of the τ_4 parameter is 0.12, which indicates a square planar geometry for the metal ($\tau_4 = 1$ for tetrahedral geometry and $\tau_4 = 0$ for square planar [43]). This is in agreement with the magnetic susceptibility measurement, which indicates the complex is diamagnetic. Bond lengths shows a considerable electronic delocalization through the thiosemicarbazone backbone, which is enhanced upon ligand deprotonation. Thus, both thione bond distances are longer than in the free ligand, with the greater change observed in the 4-methyl-3-thiosemicarbazone branch which is deprotonated. The different behavior of the two arms are reflected on the values of 1.294(5) and 1.301(5) Å for the N(3)–C(3) and N(4)–C(4) with respect to the free ligand [1.288(2)]. In addition, the bond N(2)–N(3) is longer, but N(4)–N(5) is shorter than in the free ligand. The ligand is almost planar with a maximum deviation from the least-squares-planes of 0.12 Å for C(4). Bond lengths involving the Ni(II) ion have similar values than other nickel complexes with thiosemicarbazone ligands [9,44]. There is an extended network of intermolecular hydrogen bonds involving both amino groups, the NO₃[−] and the water molecule leading to a 3D architecture.

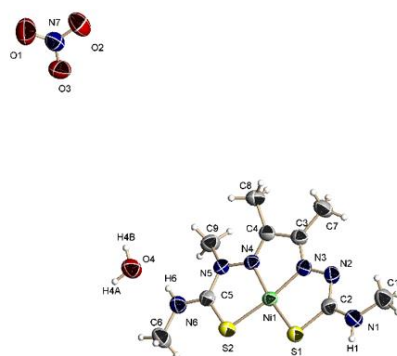


Figure 2. Molecular structure of 1·H₂O. Thermal ellipsoids at 50% probability level.

Compound 2 also crystallizes in the monoclinic P2(1)/n space group. The asymmetric unit is made up of a [Zn(MeATSM)(OH₂)]⁺ cation and a nitrate group as counterion (Figure 3). The ligand behavior is analogous to that of complex 1. In the cation, the zinc(II) ion is in a slightly distorted square-base pyramid arrangement, with $\tau_5 = 0.14$ ($\tau_5 = 1$ for a trigonal bipyramid geometry and $\tau_5 = 0$ for a square-based pyramid, [45]) with the water molecule occupying the apical position. Changes in the bond distances in the ligand skeleton upon coordination to zinc are similar to those described for complex 1. Zn(II)–N and Zn(II)–S bond lengths are in the same range of related compounds [46,47]. Both NH groups are involved in a hydrogen bond network with the nitrate group and the water molecule, leading to the formation of zig-zag ribbons in the ac plane.

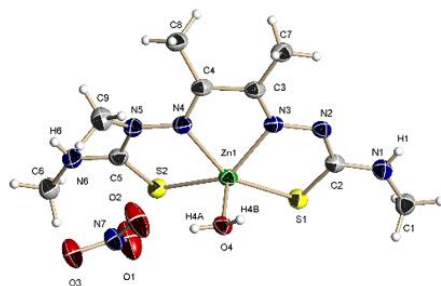


Figure 3. Molecular structure of 2. Thermal ellipsoids at 50% probability level.

The crystal structure of 3 (Figure 4) confirms the formation of a Me₂TS complex and that the symmetrization reaction takes place under reflux. It crystallizes in the monoclinic C2/c space group and the centrosymmetric complex is made up by one [Zn(Me₂TS)₂(OH₂)]²⁺ cation and two nitrate groups as counterions. In the cation, both ligands act as bidentate chelate through the sulfur atom and the primary amine, with the coordination sphere completed by a water molecule. The arrangement around the zinc(II) ion is a strongly distorted trigonal bipyramid ($\tau_5 = 0.69$), in which the equatorial positions are occupied by the two sulfur atoms and the oxygen atom with the amine groups in the axial positions. This coordination environment is not very frequent in thiosemicarbazide derivatives, which usually displays tetrahedral or octahedral environments [48,49]. The bond lengths between the metal ion and the ligand are analogous to other complexes with thiosemicarbazide ligands [49,50]. The NH groups, the nitrate ions and the water molecule participate in the formation of an extended network of hydrogen bonds leading to a 3D architecture.

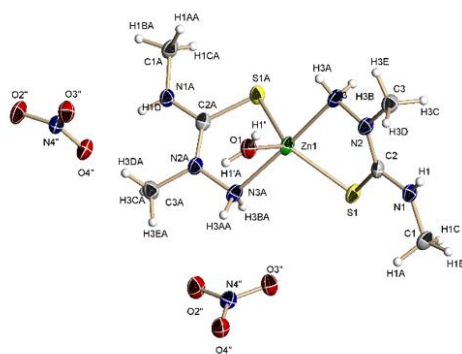


Figure 4. Molecular structure of 3. Thermal ellipsoids at 50% probability level.

3.3. Spectroscopy

The formation of HAmETS is confirmed by the presence of bands corresponding to the stretching vibrations of the amine and carbonyl groups at 3324, 3290 and 1673 cm^{-1} , respectively, together with the bands due to the imine, thioamide I and thioamide IV. The ^1H NMR spectrum shows the signals expected for the [1 + 1] condensation product and the ^{13}C NMR spectrum also confirms its structure.

The IR spectrum of HMeATSM (Figure S1) shows the absence of the carbonyl group of HAmETS and the $\delta(\text{NH}_2)$ vibration of the primary amine, that together with the additional $\nu(\text{N-H})$ and $\nu(\text{CN})$ bands indicate the formation of the dissymmetric bis(thiosemicarbazone). In the ^1H NMR spectrum, seven signals are observed, corresponding to the amine and methyl hydrogen atoms expected for the new molecule. The ^{13}C NMR (Figures S2 and S3) spectra show signals corresponding to the imine and thiocarbonyl carbon atoms and for three different methyl groups, confirming the formation of the ligand.

In the IR spectra of complexes 1 and 2, the shifts observed in the bands assigned to $\nu(\text{CN})$ and $\nu(\text{CS})$ are consistent with the imine and the thiocarbonyl groups are bonded to the metal ion, confirming that the ligand acts as a N_2S_2 donor. The spectra of all the complexes also show a band at 1384 cm^{-1} assigned to the nitrate ion. In the ^1H NMR spectrum of complex 1 (Figure S4), the signal corresponding to H_2 has disappeared due to ligand deprotonation. The spectrum of complexes 2 and 3 could not be acquired due to their decomposition in DMSO and their low solubility in other solvents. In the ^{13}C NMR spectra of complexes 1 (Figure S6) and 2 (Figure S8), the signals corresponding to the imine and thiocarbonyl carbon atoms are shifted with respect to the free ligand, supporting that the ligand is bonded through both groups in the complexes. The IR spectrum of complex 3 suggests the presence of nitrate groups and the decomposition of HAmETS, which is confirmed with the ^1H (Figure S9) and ^{13}C (Figure S10) NMR spectra that show signals consistent with the ligand symmetrization and subsequent coordination of Me_2TS .

Supplementary Materials: The following supporting information can be downloaded at: <https://www.mdpi.com/article/10.3390/cryst12030310/s1>, Figure S1: ^1H NMR spectrum in DMSO- d_6 of H HMeATSM; Figure S2: ^{13}C NMR spectrum in DMSO- d_6 of H HMeATSM; Figure S3: ^{13}C CP/MAS NMR spectrum of HMeATSM; Figure S4: ESI $^+$ spectrum of complex 1; Figure S5: ^1H NMR spectrum in DMSO- d_6 of complex 1; Figure S6: ^{13}C NMR spectrum in DMSO- d_6 of complex 1; Figure S7: ESI $^+$ spectrum of complex 2; Figure S8: ^{13}C CP/MAS NMR spectrum of complex 2; Figure S9: ^1H NMR spectrum in DMSO- d_6 of complex 3; Figure S10: ^{13}C NMR spectrum in DMSO- d_6 of complex 3.

Author Contributions: Conceptualization, E.L.-T. and M.A.M.; methodology, L.A. and R.B.; investigation L.A. and R.B.; writing—review and editing, E.L.-T. and M.A.M.; funding acquisition, E.L.-T. All authors have read and agreed to the published version of the manuscript.

Funding: This research was funded by MICINN, Instituto de Salud Carlos III, grant number PS09/00963.

Data Availability Statement: Not applicable.

Conflicts of Interest: The authors declare no conflict of interest.

References

1. Casas, J.S.; García-Tasende, M.S.; Sordo, J. Main group metal complexes of semicarbazones and thiosemicarbazones. A structural review. *Coord. Chem. Rev.* **2000**, *209*, 197–261. [[CrossRef](#)]
2. Lobana, T.S.; Sharma, R.; Bawa, G.; Khanna, S. Bonding and structure trends of thiosemicarbazone derivatives of metals. An overview. *Coord. Chem. Rev.* **2009**, *253*, 977–1055. [[CrossRef](#)]
3. Mahmoudi, G.; Zareba, J.K.; Gurbanov, A.V.; Bauzá, A.; Zubkov, F.I.; Kubicki, M.; Vladimir Stilinović, V.; Kinzhybalo, V.; Frontera, A. Benzyl dihydrazone versus thiosemicarbazone Schiff base: Effects on the supramolecular arrangement of cobalt thiocyanate complexes and the generation of CoN₆ and CoN₄S₂ coordination spheres. *Eur. J. Inorg. Chem.* **2017**, *2017*, 4763–4772. [[CrossRef](#)]
4. Salsi, F.; Portapilla, G.B.; Simon, S.; Jungfer, M.R.; Hagenbach, A.; de Albuquerque, S.; Abram, U. Effect of fluorination on the structure and anti-trypanosoma cruzi activity of oxorhenium(V) complexes with S,N,S-Tridentate thiosemicarbazones and benzoylthioureas. Synthesis and structures of technetium(V) analogues. *Inorg. Chem.* **2019**, *58*, 10129–10138. [[CrossRef](#)]
5. Mageed, A.H.; Al-Ameed, K. Synthesis, structures, and DFT analysis of gold complexes containing a thiosemicarbazone ligand. *New J. Chem.* **2021**, *45*, 18433–18442. [[CrossRef](#)]
6. Ibrahim, A.A.; Khaledi, H.; Hassandarvish, P.; Alia, H.M.; Karimian, H. Indole-7-carbaldehyde thiosemicarbazone as a flexidentate ligand toward Zn(II), Cd(II), Pd(II) and Pt(II) ions: Cytotoxic and apoptosis-inducing properties of the Pt(II) complex. *Dalton Trans.* **2014**, *43*, 3850–3860. [[CrossRef](#)]
7. García-Santos, I.; Castiñeiras, A.; Mahmoudi, G.; Babashkina, M.G.; Zangrando, E.; Gomila, R.M.; Frontera, A.; Safin, D.A. Lead(II) supramolecular structures formed through a cooperative influence of the hydrazinecarbothioamide derived and ancillary ligands. *CrystEngComm* **2022**, *24*, 368–378. [[CrossRef](#)]
8. Argibay-Otero, S.; Grana, A.M.; Carballo, R.; Vázquez-López, E.M. Synthesis of novel dinuclear N-substituted 4-(Dimethylamino)benzaldehyde thiosemicarbazones of rhenium(I): Formation of four- and/or five-membered chelate rings, conformational analysis, and reactivity. *Inorg. Chem.* **2020**, *59*, 14101–14117. [[CrossRef](#)]
9. López-Torres, E.; Mendiola, M.A.; Pastor, C.J.; Souto Pérez, B. Versatile chelating behavior of benzil bis(thiosemicarbazone) in zinc, cadmium, and nickel complexes. *Inorg. Chem.* **2004**, *43*, 5220–5230. [[CrossRef](#)]
10. Nongpiur, C.G.L.; Ghatge, M.M.; Tripathi, D.K.; Poluri, K.M.; Kaminsky, W.; Kollipara, M.R. Study of versatile coordination modes, antibacterial and radical scavenging activities of arene ruthenium, rhodium and iridium complexes containing fluorenone based thiosemicarbazones. *J. Organomet. Chem.* **2022**, *957*, 122148. [[CrossRef](#)]
11. Aygun, O.; Grzeskiewicz, A.M.; Banti, C.N.; Hadjikakou, S.K.; Kubicki, M.; Ozturk, I.I. Monomeric octahedral bismuth(III) benzaldehyde-N1-alkyl thiosemicarbazones: Synthesis, characterization and biological properties. *Polyhedron* **2022**, *215*, 115683. [[CrossRef](#)]
12. Damit, N.S.H.H.; Hamid, M.H.S.A.; Rahman, N.S.R.H.A.; Ilias, S.N.H.; Keasberry, N.A. Synthesis, structural characterisation and antibacterial activities of lead(II) and some transition metal complexes derived from quinoline-2-carboxaldehyde 4-methyl-3-thiosemicarbazone. *Inorg. Chim. Acta* **2021**, *527*, 120557. [[CrossRef](#)]
13. González-García, C.; Mendiola, M.A.; Perles, J.; López-Torres, E. Structural diversity and supramolecular architectures of Zn(II), Cd(II) and Ni(II) complexes by selective control of the degree of deprotonation of diacetyl bis(4-isopropyl-3-thiosemicarbazone). *CrystEngComm* **2017**, *19*, 1035–1044. [[CrossRef](#)]
14. Bilyj, J.K.; Harmer, J.R.; Bernhardt, P.V. Copper Complexes of Benzoylacetone Bis-Thiosemicarbazones: Metal and Ligand Based Redox Reactivity. *Aus. J. Chem.* **2020**, *74*, 34–47. [[CrossRef](#)]
15. Ilhan-Ceylan, B. Oxovanadium(IV) and nickel(II) complexes obtained from 2,2'-dihydroxybenzophenone-S-methyl-thiosemicarbazone: Synthesis, characterization, electrochemistry, and antioxidant capability. *Inorg. Chim. Acta* **2020**, *517*, 120186–120194. [[CrossRef](#)]
16. Calatayud, D.G.; López-Torres, E.; Mendiola, M.A. A Fluorescent dissymmetric thiosemicarbazone ligand containing a hydrazonequinoline arm and its complexes with cadmium and mercury. *Eur. J. Inorg. Chem.* **2013**, *2013*, 80–90. [[CrossRef](#)]
17. Cobeljic, B.; Pevec, A.; Turel, I.; Spasojevic, V.; Milcic, M.; Mitic, D.; Sladic, D.; Andjelkovic, K. Analysis of the structures of the Cu(I) and Cu(II) complexes with 3-acetylpyridine and thiocyanate. *Polyhedron* **2014**, *69*, 77–83. [[CrossRef](#)]
18. Dadashi, J.; Hanifehpour, Y.; Mirtamizdoust, B.; Abdolmaleki, M.; Jegarkandi, E.M.; Mahboubbeh, R.; Sang, W.J. Ultrasound-assisted synthesis and DFT calculations of the novel 1D Pb (II) coordination polymer with thiosemicarbazone derivative ligand and its use for preparation of PbO clusters. *Crystals* **2021**, *11*, 682. [[CrossRef](#)]
19. Zhang, H.; Zhu, H.; Zhao, H.; Dou, M.; Yin, X.; Yang, H.; Li, D.; Dou, J. A novel dinuclear cobalt-bis(thiosemicarbazone) complex as a cocatalyst to enhance visible-light-driven H₂ evolution on CdS nanorods and a mechanism discussion. *J. Photochem. Photobiol. A Chem.* **2022**, *426*, 113771. [[CrossRef](#)]
20. Du, J.; Yang, H.; Wang, C.-L.; Zhan, S.-Z. A bis(thiosemicarbazone)-zinc complex, an electrocatalyst for hydrogen evolution and oxidation via ligand-assisted metal-centered reactivity. *Appl. Organomet. Chem.* **2022**, ahead of print. [[CrossRef](#)]
21. Kostas, I.D.; Steele, B.R. Thiosemicarbazone complexes of transition metals as catalysts for cross-coupling reactions. *Catalysts* **2020**, *10*, 1107. [[CrossRef](#)]
22. Haldar, U.; Lee, H. BODIPY-derived polymeric chemosensor appended with thiosemicarbazone units for the simultaneous detection and separation of Hg(II) ions in pure aqueous media. *ACS Appl. Mater. Interfaces* **2019**, *11*, 13685–13693. [[CrossRef](#)]
23. Abbas, K.; Znad, H.; Awual, M.R. A ligand anchored conjugate adsorbent for effective mercury(II) detection and removal from aqueous media. *Chem. Eng. J.* **2018**, *334*, 432–443. [[CrossRef](#)]

24. Jaafar, A.; Platas-Iglesias, C.; Bilbeisi, R.A. Thiosemicarbazone modified zeolitic imidazolate framework (TSC-ZIF) for mercury(II) removal from water. *RSC Adv.* **2021**, *11*, 16192–16199. [[CrossRef](#)]
25. Souza, B.L.; Faustino, L.A.; Prado, F.S.; Sampaio, R.N.; Maia, P.I.S.; Machado, A.E.H.; Patrocinio, A.O.T. Spectroscopic characterization of a new Re(I) tricarbonyl complex with a thiosemicarbazone derivative: Towards sensing and electrocatalytic applications. *Dalton Trans.* **2020**, *49*, 16368–16379. [[CrossRef](#)]
26. Ismail, H.; Ahmad, M.N.; Normaya, E. A highly sensitive and selective thiosemicarbazone chemosensor for detection of Co²⁺ in aqueous environments using RSM and TD/DFT approaches. *Sci. Rep.* **2021**, *11*, 20963. [[CrossRef](#)]
27. Kumar, P.S.; Elango, K.P. A simple organic probe for ratiometric fluorescent detection of Zn(II), Cd(II) and Hg(II) ions in aqueous solution via varying emission colours to distinguish one another. *Spectrochim. Acta A Mol. Biomol. Spectrosc.* **2020**, *241*, 118610. [[CrossRef](#)]
28. Lighvan, Z.M.; Khonakdar, H.A.; Akbari, A.; Jahromi, M.D.; Ramezanzpour, A.; Kermagoret, A.; Heydari, A.; Jabbari, E. Synthesis and biological evaluation of novel tetranuclear cyclopalladated complex bearing thiosemicarbazone scaffold ligand: Interactions with double-strand DNA, coronavirus, and molecular modeling studies. *Appl. Organomet. Chem.* **2021**, *36*, e6502. [[CrossRef](#)]
29. Dilworth, J.R.; Hueting, R. Metal complexes of thiosemicarbazones for imaging and therapy. *Inorg. Chim. Acta* **2012**, *389*, 3–15. [[CrossRef](#)]
30. Paterson, B.M.; Donnelly, P.S. Copper complexes of bis(thiosemicarbazones): From chemotherapeutics to diagnostic and therapeutic radiopharmaceuticals. *Chem. Soc. Rev.* **2011**, *40*, 3005–3018. [[CrossRef](#)]
31. Rodríguez-Fanjul, V.; López-Torres, E.; Mendiola, M.A.; Pizarro, A.M. Gold(III) bis(thiosemicarbazone) compounds in breast cancer cells: Cytotoxicity and thioredoxin reductase targeting. *Eur. J. Med. Chem.* **2018**, *148*, 372–383. [[CrossRef](#)]
32. Huedo, C.; Zani, F.; Mendiola, M.A.; Pradhan, S.; Sinha, C.; López-Torres, E. Synthesis, antimicrobial activity and molecular docking of di- and triorganotin (IV) complexes with thiosemicarbazide derivatives. *Appl. Organomet. Chem.* **2019**, *33*, e4700. [[CrossRef](#)]
33. González-García, C.; Mata, A.; Zani, F.; Mendiola, M.A.; Lopez-Torres, E. Synthesis and antimicrobial activity of tetradentate ligands bearing hydrazone and/or thiosemicarbazone motifs and their diorganotin(IV) complexes. *J. Inorg. Biochem.* **2016**, *163*, 118–130. [[CrossRef](#)] [[PubMed](#)]
34. Sesmero, E.; Calatayud, D.G.; Perles, J.; López-Torres, E.; Mendiola, M.A. The reactivity of diphenyllead(IV) dichloride with dissymmetric thiosemicarbazone ligands: Obtaining monomers, coordination polymers, and an organoplumboxane. *Eur. J. Inorg. Chem.* **2016**, *2016*, 1044–1053. [[CrossRef](#)]
35. Calatayud, D.G.; López-Torres, E.; Mendiola, M.A. Synthesis of hybrid ligands derived from benzil, thiosemicarbazide and heteroaromatic hydrazides and their reactivity with Group 12 metals. *Polyhedron* **2013**, *54*, 39–46. [[CrossRef](#)]
36. Sheldrick, G.M. 1997–2001 SADABS, Version 2.03; Program for Empirical Absorption Corrections; Universität Göttingen: Göttingen, Germany, 1997.
37. Sheldrick, G.M. 1997–2001 SAINT+NT, Version 6.04; SAX Area-Detector Integration Program; Bruker AXS: Madison, WI, USA, 1997.
38. Sheldrick, G.M. 2000 SHELXTL, Version 6.10; Structure Determination Package; Bruker AXS: Madison, WI, USA, 2000.
39. Sheldrick, G.M. Phase annealing in SHELX-90: Direct methods for larger structures. *Acta Cryst. Sect. A* **1990**, *46*, 467.
40. Geary, W.J. The use of conductivity measurements in organic solvents for the characterisation of coordination compounds. *Coord. Chem. Rev.* **1971**, *7*, 81–122. [[CrossRef](#)]
41. Dayal, D.; Palanimuthu, D.; Shinde, S.V.; Somasundaram, K.; Samuelson, A.G. A novel zinc bis(thiosemicarbazone) complex for live cell imaging. *J. Biol. Inorg. Chem.* **2011**, *16*, 621. [[CrossRef](#)]
42. Holland, J.P.; Aigbirhio, F.I.; Betts, H.M.; Bonnitcho, P.D.; Burke, P.; Christlieb, M.; Churchill, G.C.; Cowley, A.R.; Dilworth, J.R.; Donnelly, P.S.; et al. Functionalized bis(thiosemicarbazone) complexes of zinc and copper: Synthetic platforms toward site-specific radiopharmaceuticals. *Inorg. Chem.* **2007**, *46*, 465. [[CrossRef](#)]
43. Yang, L.; Powell, D.R.; Houser, R.P. Structural variation in copper(I) complexes with pyridylmethylamide ligands: Structural analysis with a new four-coordinate geometry index, τ_4 . *Dalton Trans.* **2007**, 955–964. [[CrossRef](#)]
44. Balachandran, C.; Haribabu, J.; Jeyalakshmi, K.; Bhuvanesh, N.S.P.; Karvembu, R.; Emi, N.; Awale, S. Nickel(II) bis(isatin thiosemicarbazone) complexes induced apoptosis through mitochondrial signaling pathway and G0/G1 cell cycle arrest in IM-9 cells. *J. Inorg. Biochem.* **2018**, *182*, 208. [[CrossRef](#)] [[PubMed](#)]
45. Addison, A.W.; Rao, T.N.; Reedijk, J.; van Rijn, J.; Verschoor, G.C. Synthesis, structure, and spectroscopic properties of copper(II) compounds containing nitrogen–sulphur donor ligands; the crystal and molecular structure of aqua[1,7-bis(N-methylbenzimidazol-2'-yl)-2,6-dithiaheptane]copper(II) perchlorate. *J. Chem. Soc. Dalton Trans.* **1984**, *7*, 1349–1356. [[CrossRef](#)]
46. Bal-Demirci, T. Synthesis, spectral characterization of the zinc(II) mixed-ligand complexes of N(4)-allyl thiosemicarbazones and N,N,N',N'-tetramethylethylenediamine, and crystal structure of the novel [ZnL2(tmen)] compound. *Polyhedron* **2008**, *27*, 440. [[CrossRef](#)]
47. Calatayud, D.G.; López-Torres, E.; Mendiola, M.A.; Pastor, C.J.; Procopio, J.R. Structural diversity in divalent benzil bis(thiosemicarbazone) complexes. *Eur. J. Inorg. Chem.* **2005**, *2005*, 4401–4409. [[CrossRef](#)]
48. Tong, Y.-X.; Su, C.-Y.; Zhang, Z.-F.; Kang, B.-S.; Yu, X.-L.; Chen, X.-M. Bis(thiosemicarbazide-S,N)zinc(II) dinitrate. *Acta Cryst. C* **2000**, *56*, 44. [[CrossRef](#)]

-
49. Babb, J.E.V.; Burrows, A.D.; Harrington, R.W.; Mahon, M.F. Zinc thiosemicarbazide dicarboxylates: The influence of the anion shape on supramolecular structure. *Polyhedron* **2003**, *22*, 673–686. [[CrossRef](#)]
 50. Li, S.-L.; Wu, J.-Y.; Tian, Y.-P.; Fun, H.-K.; Chantrapromma, S. Bis(thio-semicarbazide)zinc(II) bis-(maleate) dihydrate. *Acta Cryst. E* **2005**, *61*, m2701. [[CrossRef](#)]